

Supplemental Data for Gupta et al.

Domain-specific Antibodies Reveal Differences in the Membrane Topologies of Apolipoprotein L1 in Serum and Podocytes.

Supplemental Table of Contents

Supplemental Appendix 1. Details of antibody mapping.
Supplemental Table 1: Methods of antibody generation.
Supplemental Table 2. Transmembrane prediction program results.
Supplemental Figure 1. The APOL1 immunogen is functional.
Supplemental Figure 2. Most antibodies recognize APOL1 on gD- <i>iAPOLI</i> -GPI CHO cells.
Supplemental Figure 3. Successful generation of <i>APOLI</i> KO podocytes by CRISPR/Cas9.
Supplemental Figure 4. <i>iAPOLI</i> podocytes express APOL1 in a dose-dependent manner.
Supplemental Figure 5. MAD antibodies can detect intracellular but not cell surface APOL1.
Supplemental Figure 6. The MAD is inaccessible in human cell lines.
Supplemental Figure 7. Antibody blockade of trypanolysis is dose-dependent.
Supplemental Figure 8. Immunoprecipitation of APOL1 from NHS with a different set of APOL1 antibodies confirms only blockers immunoprecipitate APOL1.
Supplemental Figure 9. Lack of correlation between surface APOL1 recognition and trypanolytic blockade by anti-APOL1 antibodies.
Supplemental Figure 10. Eleven anti-APOL1 antibodies were precisely mapped by SPR on overlapping peptides spanning the length of APOL1.
Supplemental Figure 11. Successful epitope mapping of 18 anti-APOL1 antibodies by western blotting of short overlapping peptides covering the whole protein.

Supplemental Details of Antibody Domain Mapping.

Since any one given method was not optimal for all the antibodies tested, data from different approaches (Supplemental Figures 10 and 11) were combined to understand antibody domains (in Figures 7 and 9). For mapping by Western blotting, FLAG-tagged *APOL1* truncation constructs (61-203 aa, 92-321 aa, 61-260 aa, and 88-321 aa) were expressed in Sf9 cells and purified as described for full length APOL1 in Supplemental Figure 1C. For brevity, “binders” refer to podocyte FACS positive antibodies, while “blockers” refer to trypanolysis blockers (i.e. serum APOL1 binders). Because our immunogen lacked the first 60 aa, there were of course no antibodies to this region. In the PFD, two binding non-blockers and weak blocker (5.11H2 and 5.17H8) mapped to aa 61-92 (Supplemental Figure 11E), implying that this region is exposed in podocytes but not in serum APOL1 (Figure 7). Furthermore, two of the top blockers, 3.6D12 and 3.7D6, also good podocyte binders, mapped to 2 distinct regions, between aa 101-130 and 151-172 (Supplemental Figures 10A and 11B). Most of our other antibodies recognizing region 111-150 were non-blockers and binders (Supplemental Figure 9), with the exception of three antibodies. No antibodies mapped to aa 170-240, we speculate perhaps because the two predicted transmembrane domains (aa 177-196 and 204-224)¹ may have been buried in the antigen.

Only 2 MAD binders were successfully cloned (3.3A8 and one antibody not shown due to lack of binding and blocking). Three blocking non-binders (1.11G1, 3.3A8, 4.6A9) mapped to the C-terminal half of the MAD (aa 260-305; Supplemental Figure 11F), indicating that this region is exposed in serum but not on podocytes. In contrast 4.12F4 and 3.5H9 (which could not be cloned) mapped to the N-terminus of the MAD (235-260; Supplemental Figure 11C,F), but were negative for both binding and blocking, suggesting this domain may be buried in both cases. Thus, the whole MAD is buried in podocytes, but the C-terminal portion is exposed in serum.

Most SRA-ID binders actually mapped to the linker region between the MAD and SRA-ID (aa 306-339; Supplemental Figures 10B and 11D), only nine recognizing the SRA-ID proper, seven of which don't recognize APOL1-G2 (Figure 2, C and D) and indeed mapped to the very C-terminal peptide (aa 376-398). 4.29C4, which failed to bind or block, bound to peptide 364-385, suggesting this region is buried, in accordance with a predicted coiled coil there.¹ Of the linker domain antibodies, all those adjacent to the MAD (aa 284-313) recognized only serum APOL1. Three antibodies mapping to aa 314-333 were able to bind and block, while 2 weak/non-binding blockers mapped to aa 324-333. Thus, most of the linker (aa 303-330) is exposed in serum APOL1, but aa 306-313 is inaccessible in podocytes. However, the very C-terminus of

the SRA-ID is readily accessible in both serum and surface APOL1. Due to lack of antibodies to other regions of APOL1 we cannot confidently predict the complete topology of APOL1, but assuming the three predicted transmembrane domain regions are correct,¹ a working model is presented in Figure 9.

Supplemental References

1. Thomson, R.; Genovese, G.; Canon, C.; Kovacsics, D.; Higgins, M. K.; Carrington, M.; Winkler, C. A.; Kopp, J.; Rotimi, C.; Adeyemo, A.; Doumatey, A.; Ayodo, G.; Alper, S. L.; Pollak, M. R.; Friedman, D. J.; Raper, J., Evolution of the primate trypanolytic factor APOL1. *Proc Natl Acad Sci U S A* **2014**, *111* (20), E2130-9.
2. Thomson, R.; Finkelstein, A., Human trypanolytic factor APOL1 forms pH-gated cation-selective channels in planar lipid bilayers: relevance to trypanosome lysis. *Proc Natl Acad Sci U S A* **2015**, *112* (9), 2894-9.
3. Cooper, A.; Capewell, P.; Clucas, C.; Veitch, N.; Weir, W.; Thomson, R.; Raper, J.; MacLeod, A., A Primate APOL1 Variant That Kills *Trypanosoma brucei gambiense*. *PLoS Negl Trop Dis* **2016**, *10* (8), e0004903.

Supplemental Table 1: Methods of antibody generation.

Immunization Method (and Ab prefix)	Antigen or Antigen encoding DNA	Method (host species)	ELISA-positive Antibodies
1	<i>APOL1-G1</i> and <i>G2</i> DNA	HTV (mouse)	3
2	<i>APOL1-G1</i> and <i>G2</i> DNA	GeneGun (mouse)	1
3	His ₆ -APOL1-G0 protein	I.V. (mouse)	105
4	His ₆ -APOL1-G0 protein +SRA-ID-G0 boost	I.V. (mouse)	26
5	His ₆ -APOL1-G0 protein	I.V. (rabbit)	35

Total = 170

Attempts to generate APOL1 variant-specific antibodies (Ab) using *APOL1-G1* and *G2* cDNAs injected into mice were not very successful, yielding only four weakly APOL1-binding monoclonals that bound APOL1-G0 in addition to the variants (Methods 1 & 2). Injection of his₆-APOL1 protein (Methods 3-5) yielded better results (see Methods for details). See Scales et al. (this issue) for details of rabbit monoclonal generation (Method #5) and Supplemental Figure 1 for characterization of the his₆-APOL1-G0 immunogen.

Supplemental Table 2. Transmembrane prediction program results.

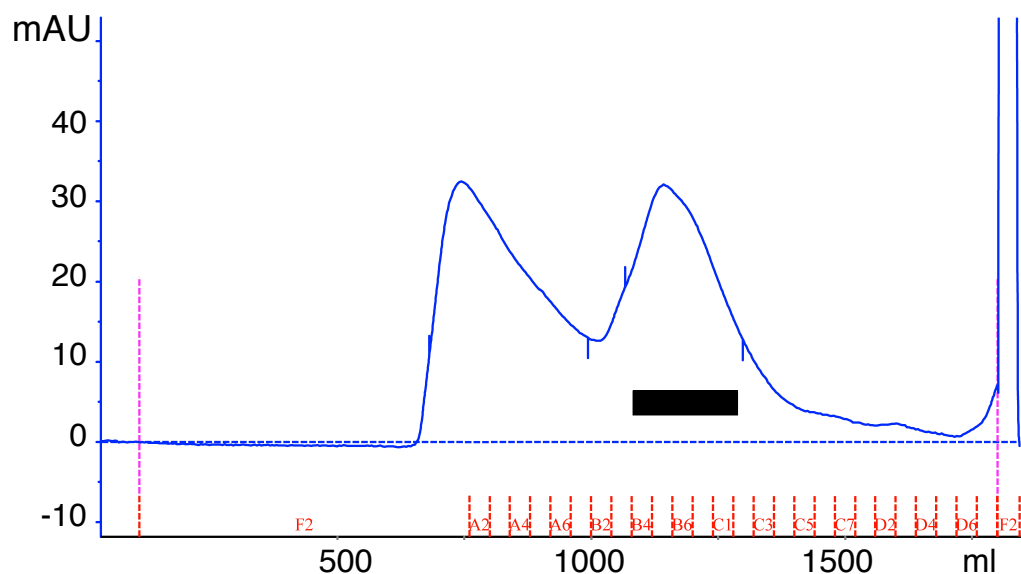
Model	# tm*	Tm1	Tm2	Tm3	Tm4	Fits FACS data?
DAS server	3	177-197	(183-222)	338-353		Only if tm3 is a hairpin loop
DAS/cgi	2	184-193	341-351			No, MAD is not intracellular† and linker is exposed
TMHMM	1	177-199				No, PFD and C-terminus are both exposed
TMpred	2	177-196	332-353			No, MAD is not intracellular† and linker is exposed
TMpred	4	177-196	(212-230)	(257-276)	332-353	No, linker is exposed
SPLIT server	3	175-196	(200-224)	338-354		Only if tm3 is a hairpin loop

* The N-terminal signal sequence is not counted as a transmembrane domain
Amino acids are colored according to domain: PFD in blue, MAD in green, linker (exposed portion is 314-333 in podocytes) in black and SRA-ID in red. Parentheses indicate a weak tm prediction.

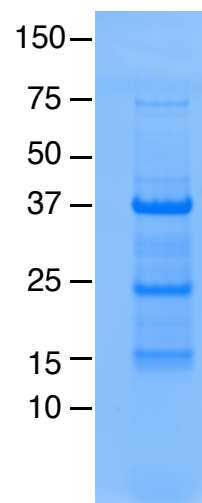
† Although the MAD is not exposed in podocytes or other human cell lines tested (see Supplemental Figure 6), it is in CHO cells, thus we hypothesize it is not intracellular or buried in the membrane, but instead bound to another protein in human cell lines, since it is unlikely that the transmembrane domain arrangement would fundamentally differ between species. See Figure 9 for working model with 2 full transmembrane domains and a hairpin (semi) loop for tm3.

Supplemental Figure 1

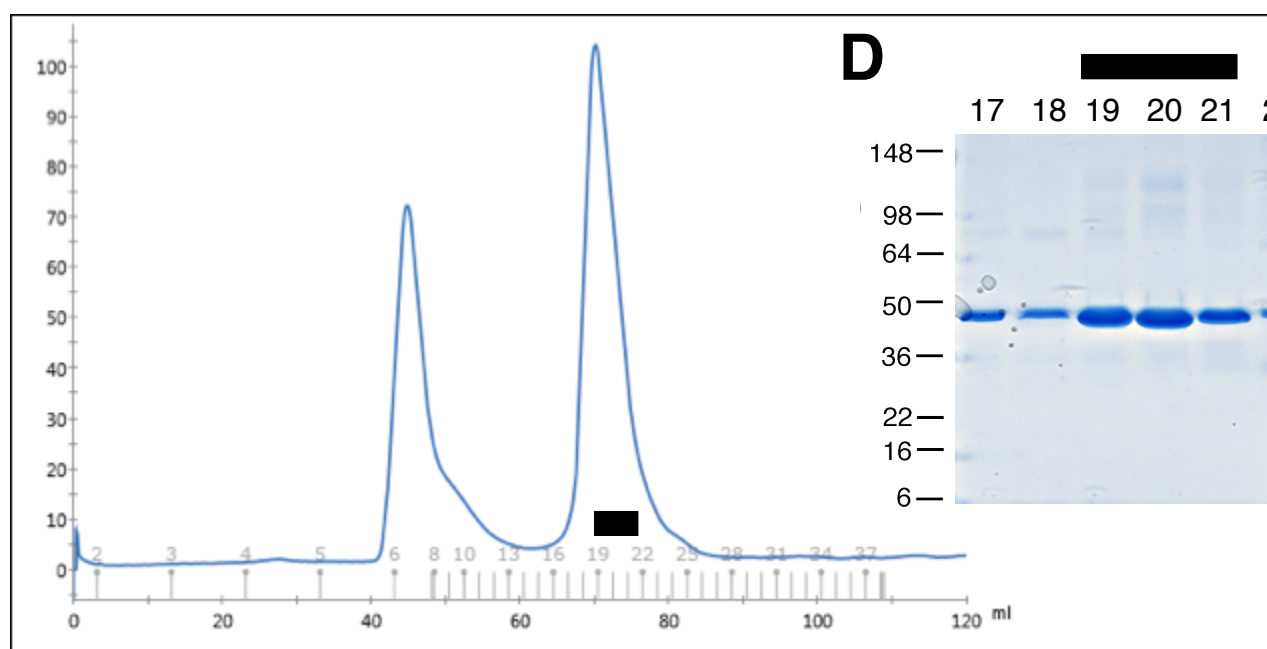
A



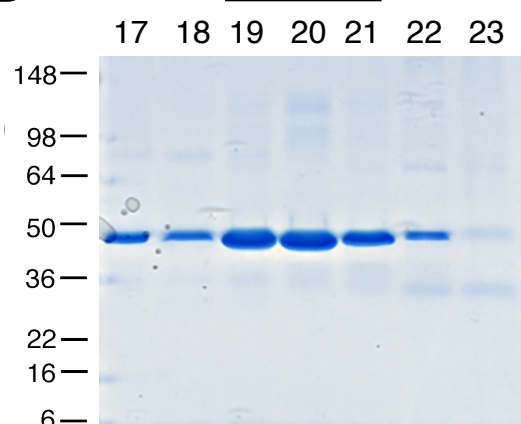
B



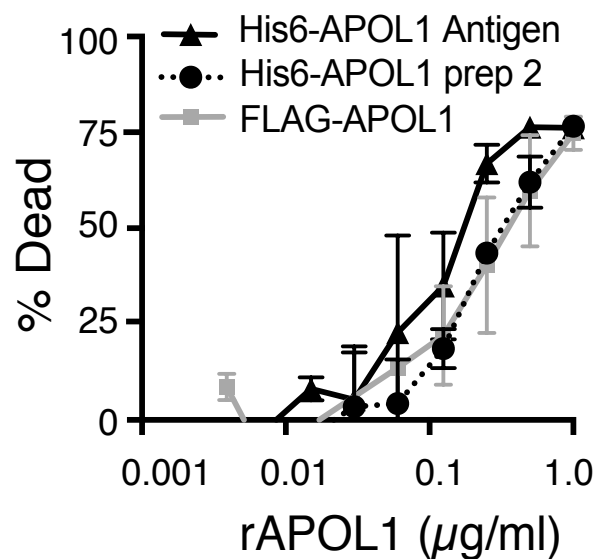
C



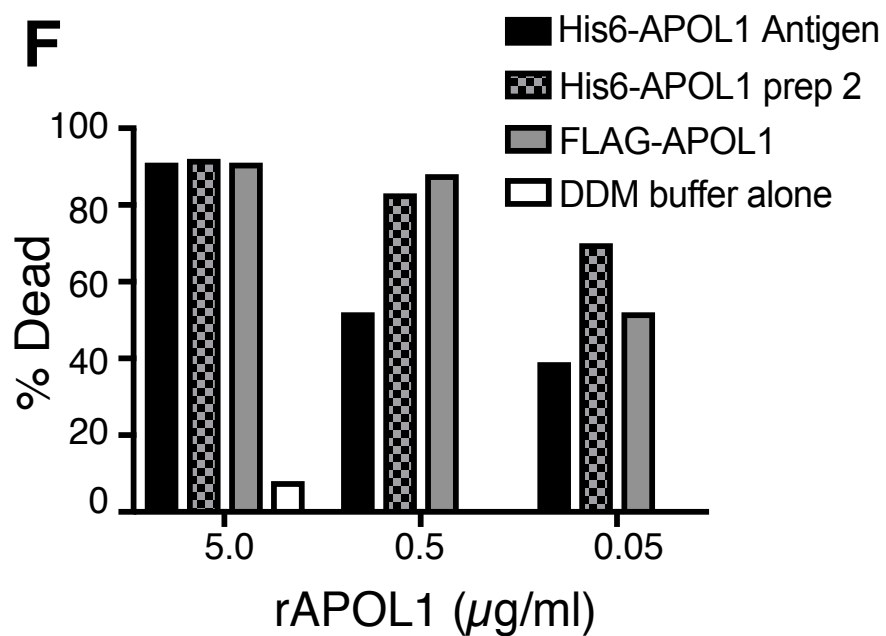
D



E



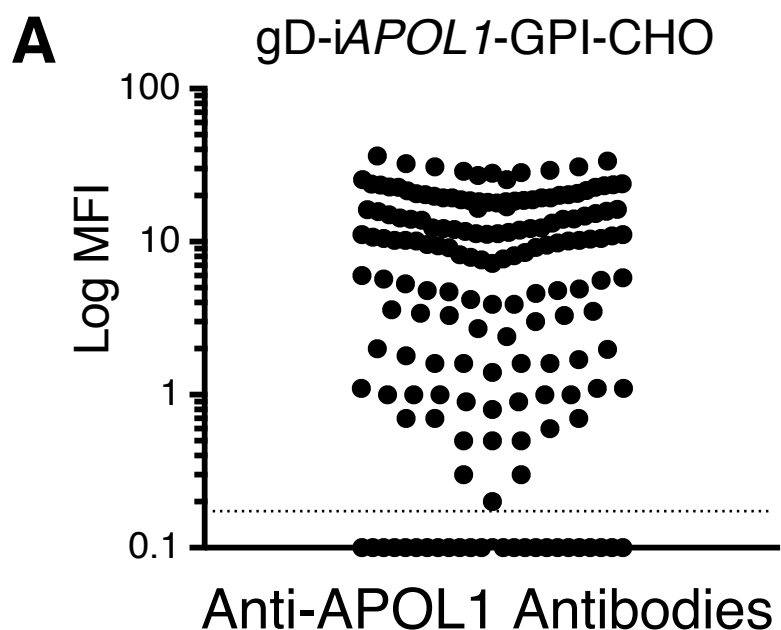
F



Supplemental Figure 1. The APOL1 immunogen is functional.

- A) S200 column purification of his₆-APOL1 antigen. NiNTA-purified his₆-APOL1 was fractionated on a large S200 column in the presence of 0.1% DDM. The main peak at 1142 ml corresponds to full length monomer. Fractions B4-C1 (black rectangle) were pooled for characterization and immunization.
- B) SDS-PAGE gel of final pooled fractions B4-C1 of his₆-APOL1 antigen. Samples were boiled in reducing sample buffer and run on a Bolt 4-20% Bis-Tris PLUS gel in Bis-Tris SDS buffer, followed by Coomassie Blue staining. The major 37 kDa band represents full length his₆-APOL1, with cleavage products at 24 and 16 kDa.
- C) S200 column purification of FLAG-APOL1 used for trypanolytic assays. FLAG-APOL1 purified with an anti-FLAG antibody column was fractionated on an S200 column in the presence of 0.026% DDM. The main peak at 70 ml corresponds to full length monomer and the black rectangle denotes fractions 19-21 that were pooled for use in trypanolysis assays.
- D) Coomassie Blue stained 4-20 % Tris-Glycine SDS-PAGE gel of the S200 fractions of FLAG-APOL1 protein in (C), showing one major band corresponding to full length protein (due to an improved purification protocol that minimized degradation compared to the earlier his₆-tagged prep in (B)). Fractions 19-21 (black rectangle) were pooled for use. Molecular weight markers were See Blue Plus 2 (Invitrogen LC5625), so APOL1 appears at around 41 kDa on this gel.
- E) Recombinant APOL1 (rAPOL1) is active at killing trypanosomes. Three different preps, all formulated in buffer containing 0.026% DDM, were compared for trypanolytic activity. Dilution series of initial (degraded) his₆-APOL1 antigen prep (from A; black solid line), a subsequent (improved, less degraded) his₆-APOL1 prep, used for trypanolysis assays (black dotted line) and FLAG-APOL1 (from C,D; grey solid line) incubated with *Trypanosoma brucei brucei* showing dose-dependent lytic activity of the recombinant protein in the Alamar Blue assay. Although all preps showed variability between assays, likely due to loss of activity every freeze-thaw, the mean IC₅₀s were all similar at 100-200 ng/ml, a little higher than previous reports.^{2,3} The y-axis denotes the percentage of dead trypanosomes calculated by (100 - % alive). % Alive is calculated as in Figure 6.
- F) Trypanosome lysis is due to recombinant APOL1 and not DDM, since equivalent volumes of DDM buffer alone (white) do not result in trypanosome death.

Supplemental Figure 2

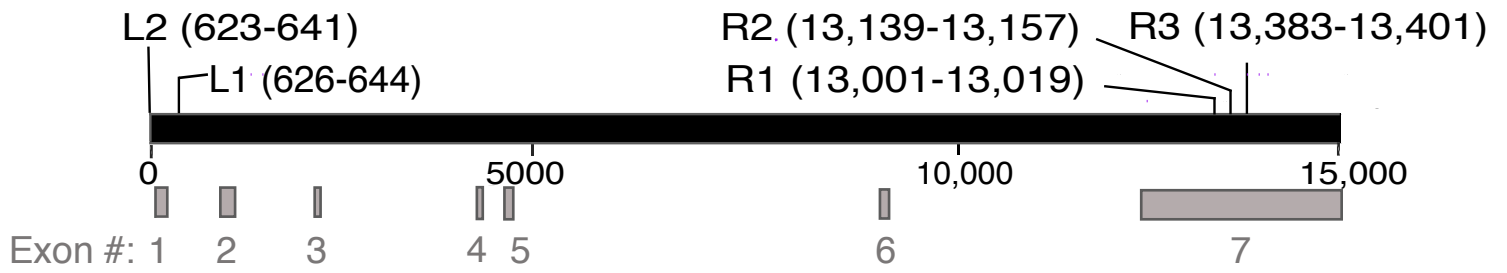


Supplemental Figure 2. Most antibodies recognize APOL1 on gD-iAPOL1-GPI CHO cells.

Flow cytometry with all 170 antibodies on full length gD-iAPOL1-G0-GPI (construct b in Figure 1A). The y-axis denotes the Mean Fluorescence Intensity (MFI, log scale). Each dot represents an individual antibody. The 150 FACS-positive antibodies (88%) are above the dotted line and the 20 negative antibodies (12%) are below the dotted line.

Supplemental Figure 3

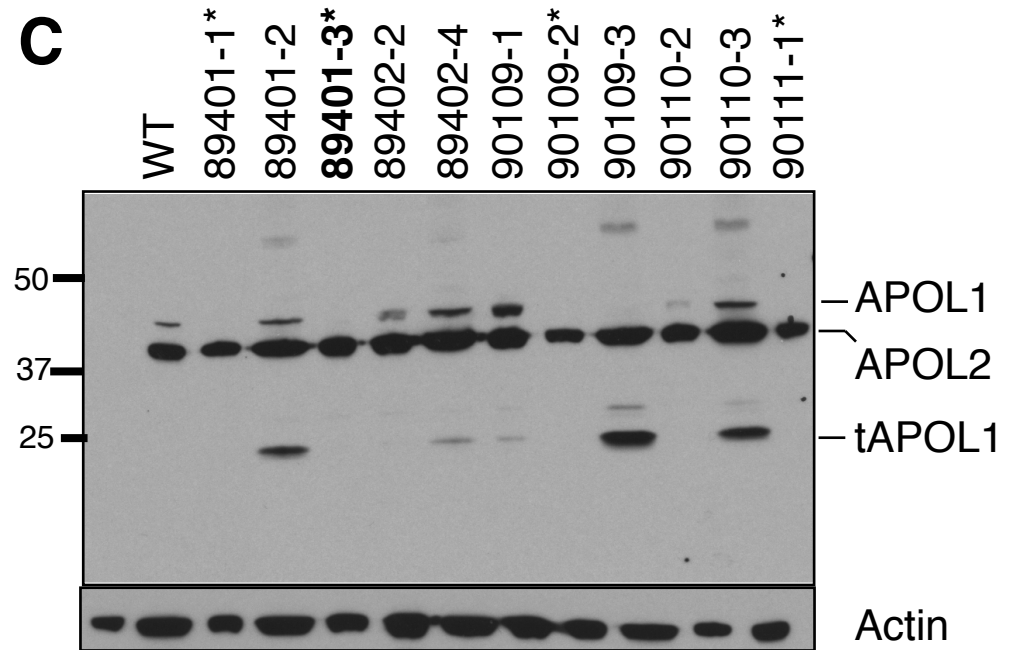
A



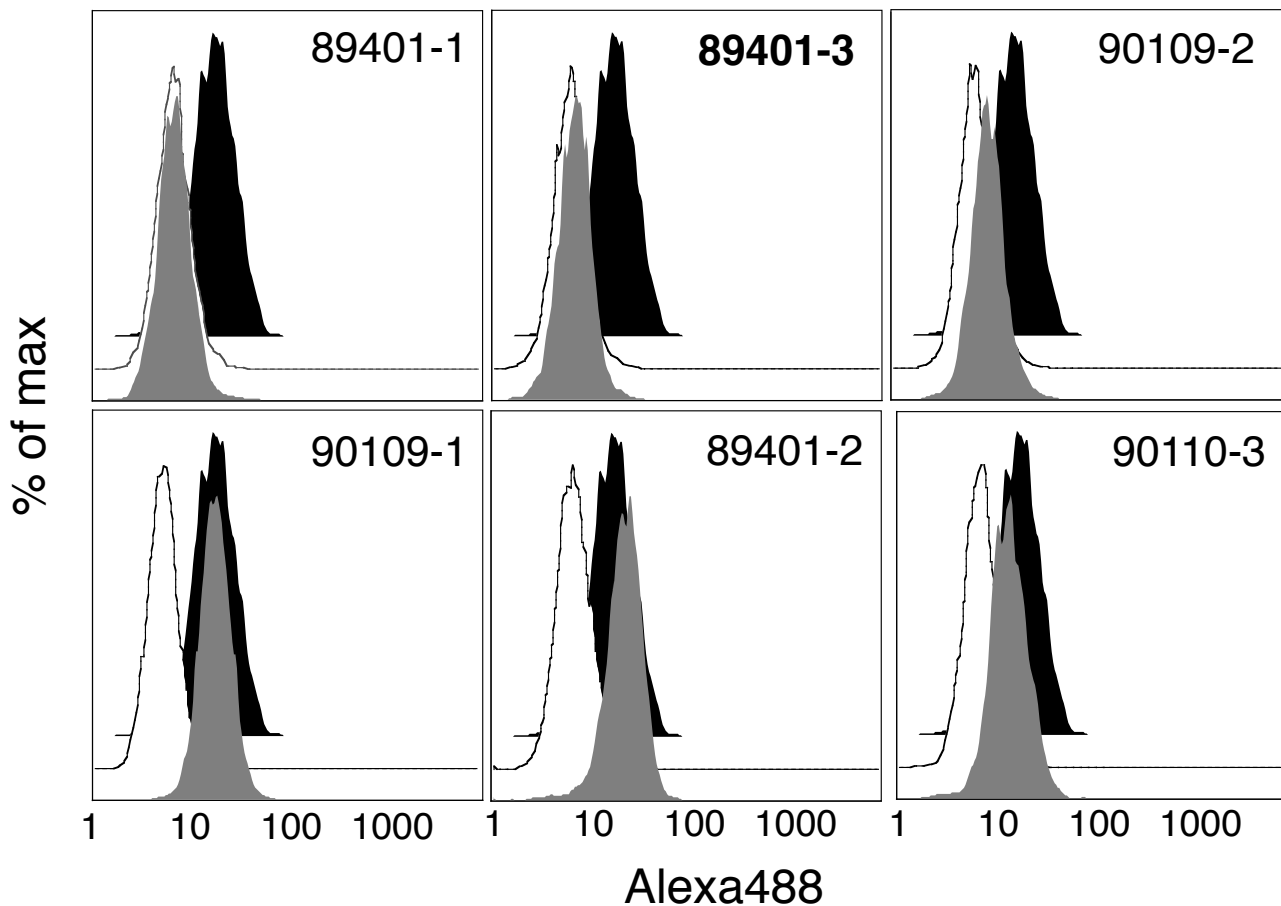
B

gRNA #	gRNA pair
89401	L2, R3
89402	L2, R4
90109	L1, R2
90110	L1, R4
90111	L2, R2

C



D



Supplemental Figure 3. Successful generation of *APOL1* KO podocytes by CRISPR/Cas9.

A) Schematic representation of the paired guide RNA locations targeting exon 1 and exon 7 on the whole *APOL1* genomic locus to attempt *APOL1* knockout by homologous recombination.

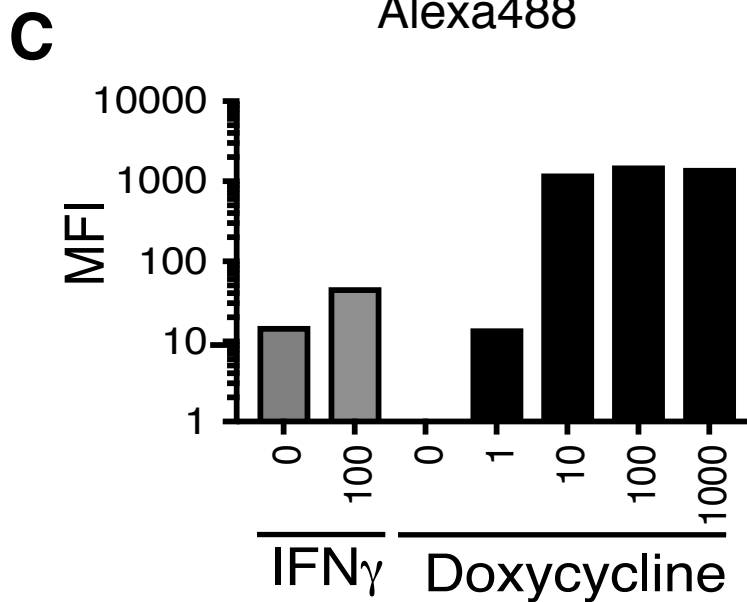
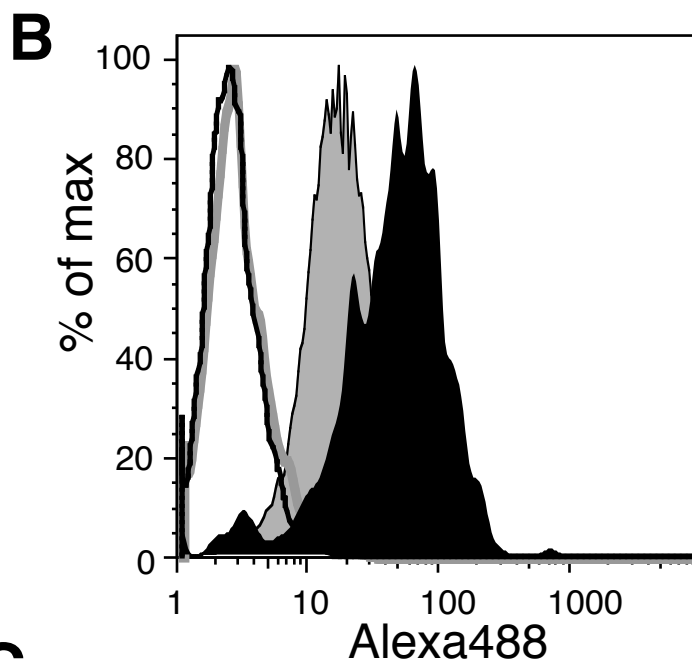
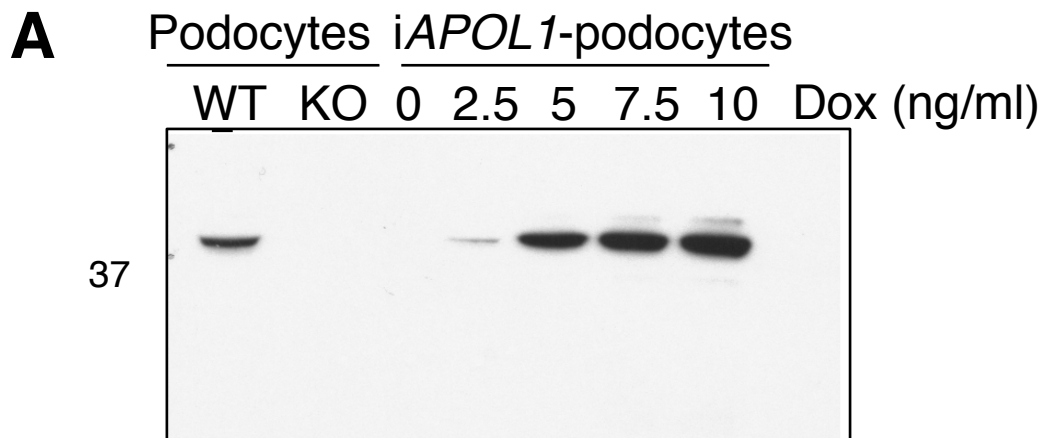
The guide positions in nucleotides are indicated in parentheses. L is left, R is right.

B) The gRNA pairs used per transfection are shown, each pair indicated by a number. Cell lines are named after their respective gRNA pairs.

C) Western blot of 11 single cell clones, obtained from individual transfections, with Proteintech polyclonal anti-APOL1. Asterisks indicate clones that showed complete loss of APOL1 (89401-1, 89401-3, 90109-2 and 90111-1; genomic data not shown), while two clones retained full length APOL1 (89402-2 and 90110-2). Five clones were rejected due to expression a truncated form of APOL1 (tAPOL1), with or without full length APOL1. As intended, none of the clones were completely knocked out for *APOL2*, although further western blot analysis suggested one allele might be lost in 89401-3 (see Figure 4B and Scales et al. Figure 2). Actin served as a loading control.

D) Flow cytometry with antibody 3.7D6 of selected single cell *APOL1* KO podocyte clones show loss (i.e. successful knockout; top row) or presence (failed knockout; bottom row) of APOL1 on the surface (grey histograms) as compared to parental WT podocytes (black histograms); white histograms are Alexa488 anti-mouse secondary antibody alone. Clone 89401-3 (**bold**) was selected for further studies due to more similar morphology and growth rate to the parental cells.

Supplemental Figure 4



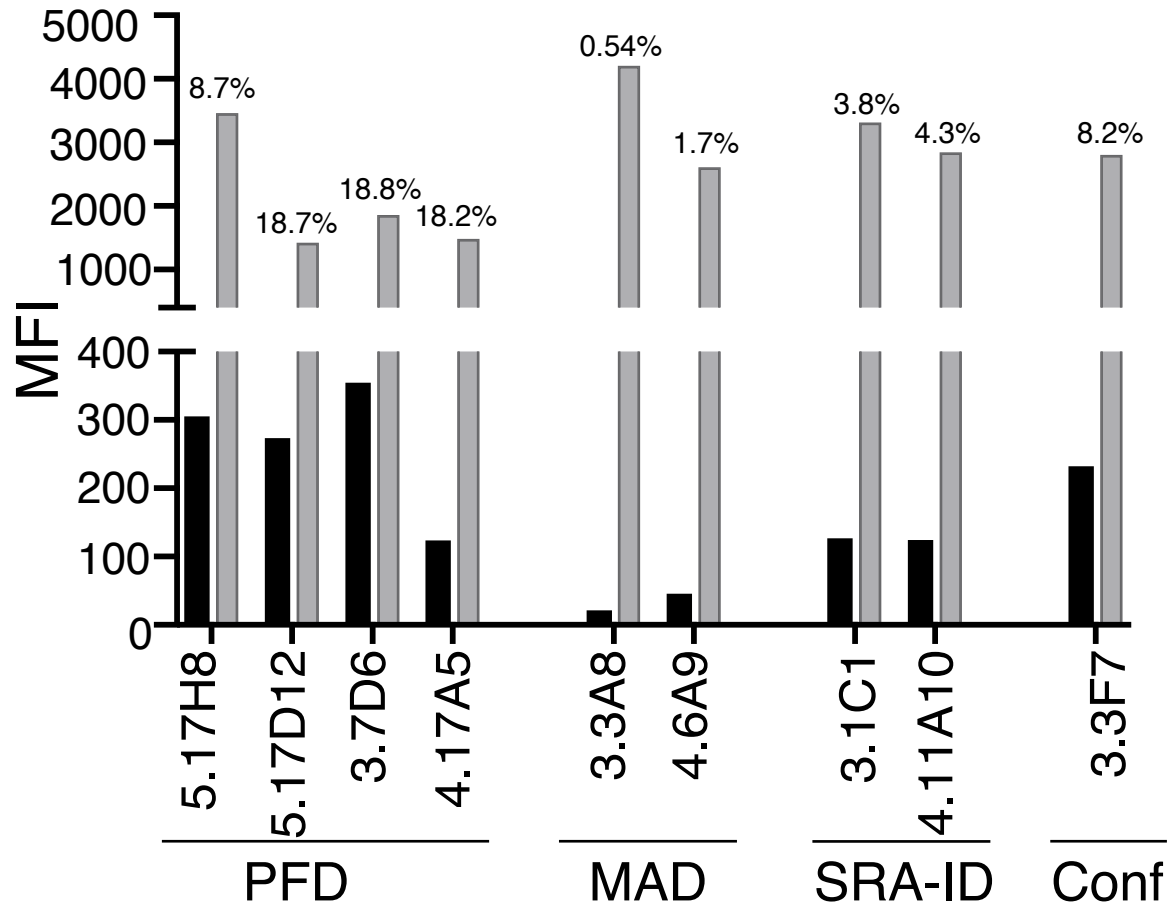
Supplemental Figure 4. *iAPOL1* podocytes express APOL1 in a dose-dependent manner.

A) Western Blot (with 0.04 µg/ml rabbit 3.1C1 and 3.7D6 mixture) of APOL1 expression in lysates on 4-12% Bis-Tris gels of WT and *APOL1* KO podocytes (both after 24 h IFN γ) versus *iAPOL1-G0* podocytes \pm doxycycline stimulation (16 h). 10-fold higher expression than WT+IFN γ is seen after treatment with 10 ng/ml Dox for 16 h.

B) Surface APOL1 expression by flow cytometry is 10-fold higher in *iAPOL1-G0* podocytes (solid black; induced for 24 h with 5 ng/ml dox) than WT (grey; 24 h induced with 100 ng/ml IFN γ) using 1 µg/ml 3.7D6 antibody. *APOL1* KO (black line) is completely negative, overlapping with Alexa488 anti-mouse secondary alone (grey line) as expected. A representative histogram from 3-4 experiments is shown.

C) Flow cytometry of surface APOL1 in *iAPOL1-G0* podocytes (black bars) at increasing doxycycline concentrations (in ng/ml), showing it saturates at 10 ng/ml of dox, with 1 ng/ml producing levels similar to endogenous non-IFN γ -stimulated podocytes (grey bars). 10 ng/ml dox was selected for future experiments. Representative data from 3 experiments is shown. The y-axis is log MFI.

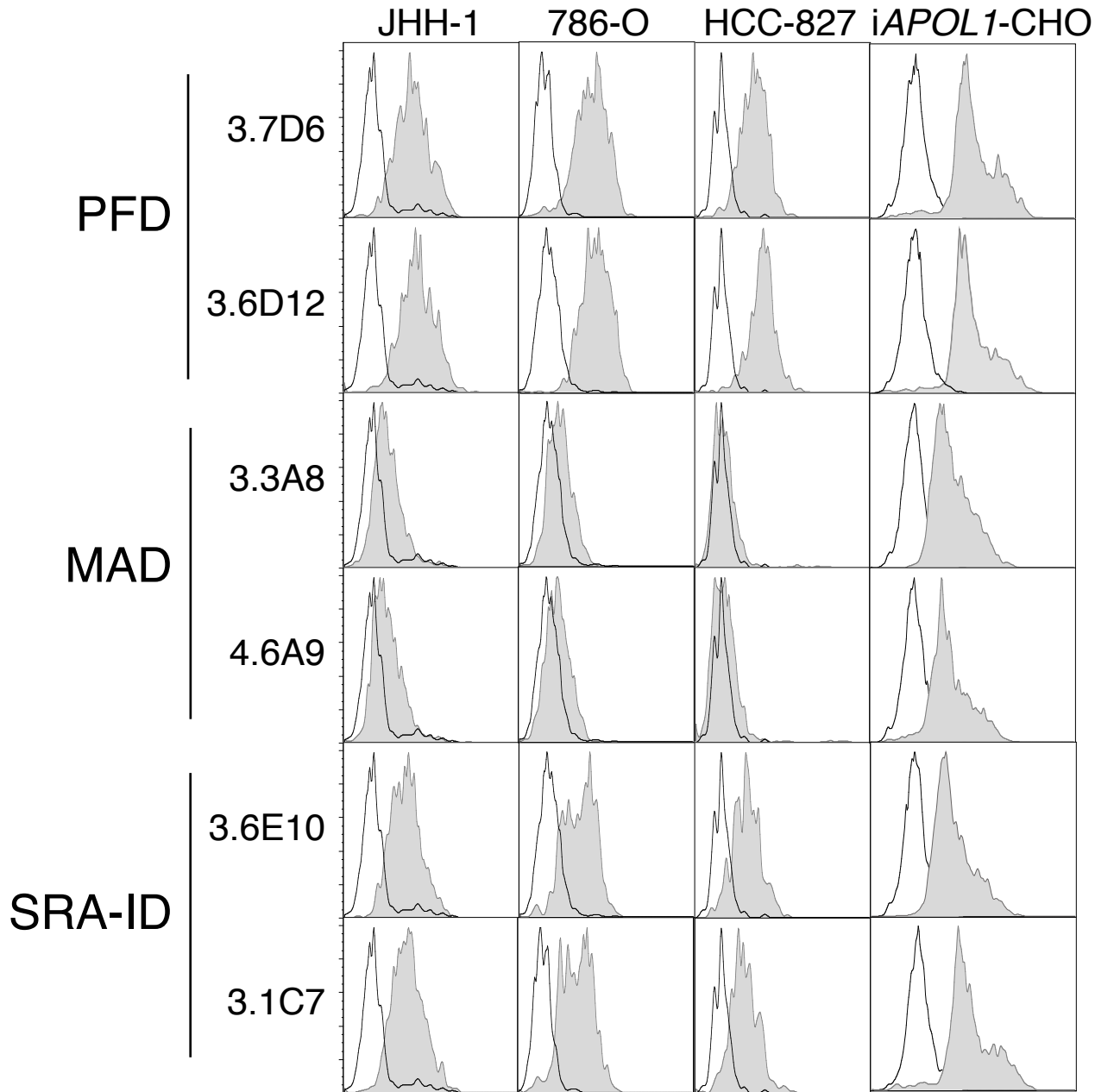
Supplemental Figure 5



Supplemental Figure 5. MAD antibodies can detect intracellular but not cell surface APOL1.

Mean fluorescence intensity (MFI) data of fixed and saponin-permeabilized (grey) versus live non-permeabilized (black) *iAPOL1* podocytes induced with 100 ng/ml IFN γ for 24 h and stained with 9 representative antibodies is plotted. The numbers on top of the bars indicate % of APOL1 on cell surface, calculated by the ratio of cell surface (unpermeabilized) vs total (permeabilized) APOL1 MFIs. Note that this is only a crude estimate because fixation may alter antibody binding to different extents. The MAD antibodies 3.3A8 and 4.6A9 cannot detect surface APOL1 on unpermeabilized podocytes, but can detect intracellular APOL1 on permeabilized podocytes (Scales et al. Figure 6B and data not shown), as well as on live unpermeabilized *iAPOL1*-CHO cells (grey triangle in Figure 2B). This experiment was analyzed on a FACSCelesta, which gives higher readings than the instrument used in the other experiments.

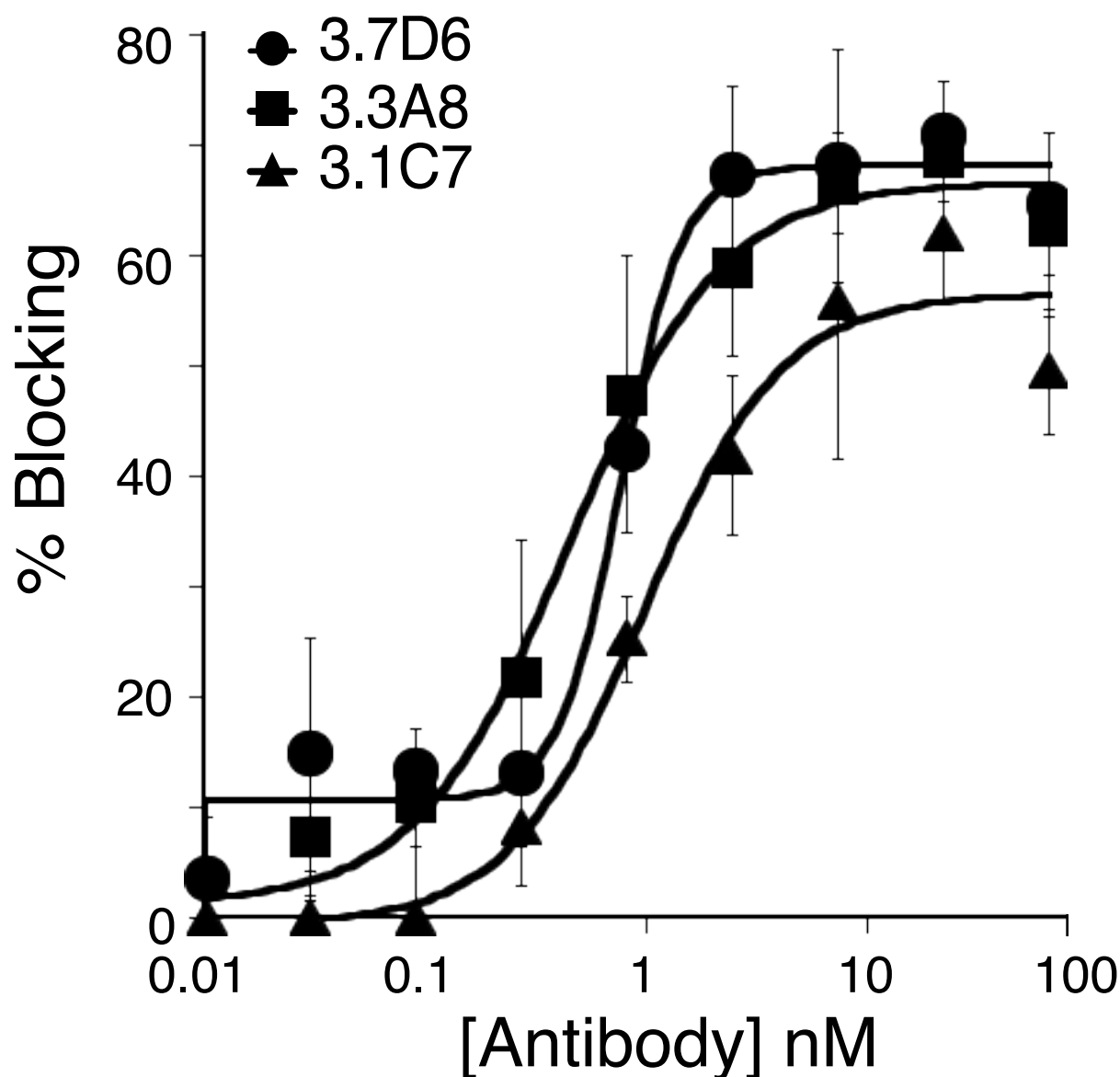
Supplemental Figure 6



Supplemental Figure 6. The MAD is inaccessible in human cell lines.

Flow cytometry with antibodies to different domains on JHH-1 (liver), 786-O (kidney) and HCC827 (lung) cells treated with 100 ng/ml IFN γ for 48 h, all show similar patterns of endogenous APOL1 exposure as podocytes (endogenous and stably transfected; Figure 5A,B), whereas iAPOL1-CHO cells treated with 10 μ g/ml dox for 48 h, have a more accessible MAD domain (larger shift with antibodies 3.3A8 and 4.6A9).

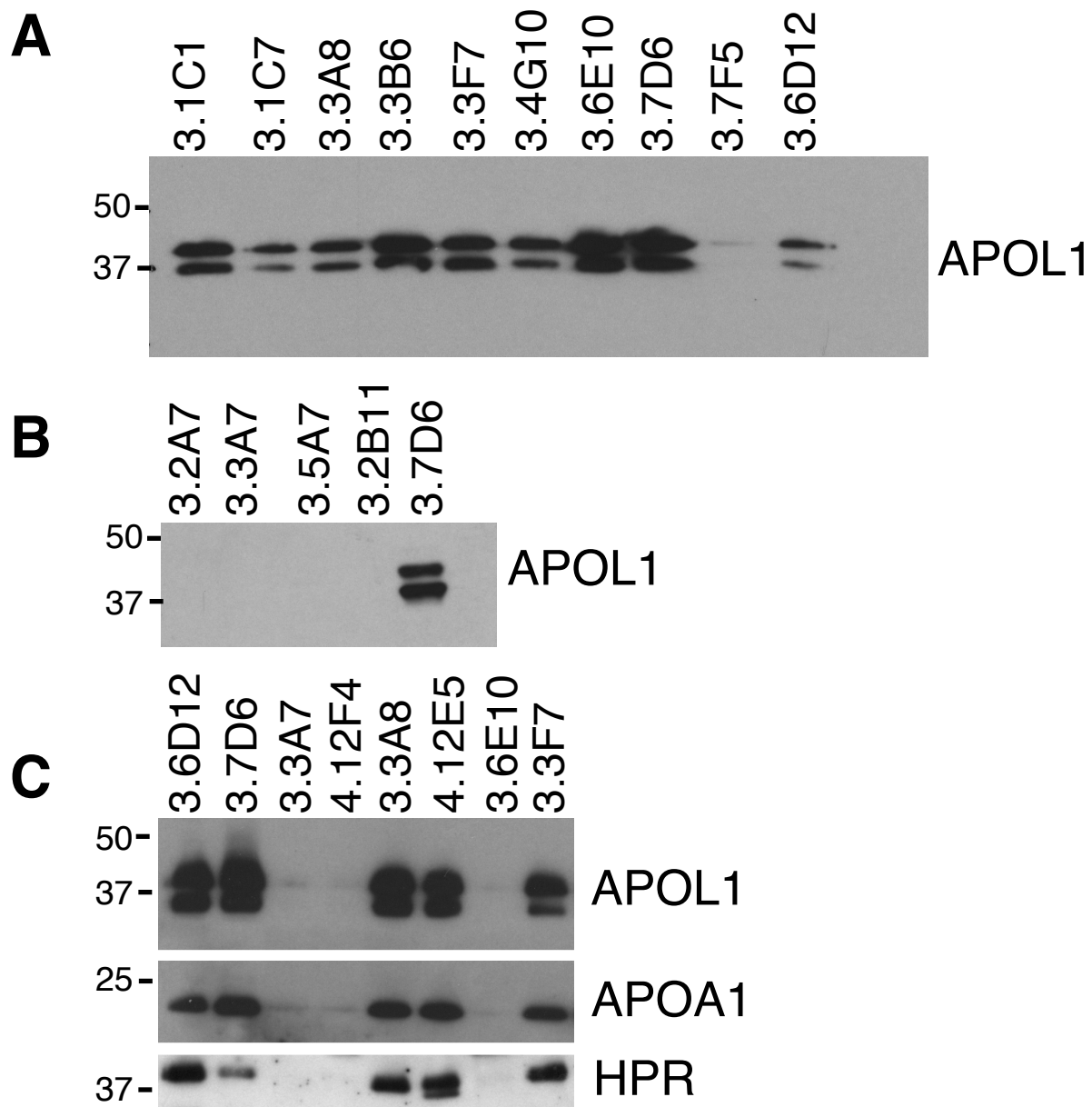
Supplemental Figure 7



Supplemental Figure 7. Antibody blockade of trypanolysis is dose-dependent.

Anti-APOL1 antibody dose titration was performed in the trypanosome blocking assay with one of the top blocking antibodies for each domain: PFD antibody 3.7D6 (circles; IC_{50} 0.5 nM); MAD antibody 3.3A8 (squares; IC_{50} 0.4 nM); and SRA-ID antibody 3.1C7 (triangles; IC_{50} 1nM). Live trypanosomes were measured using the Alamar Blue assay and % blocking calculated by normalizing values to no antibody control sample as in Figure 6C. The means and SDs of 3 independent experiments are plotted. IC_{50} s were calculated in KaleidaGraph v4.1 using the equation $y = m1/(1+(m2/m0)^{m3})$.

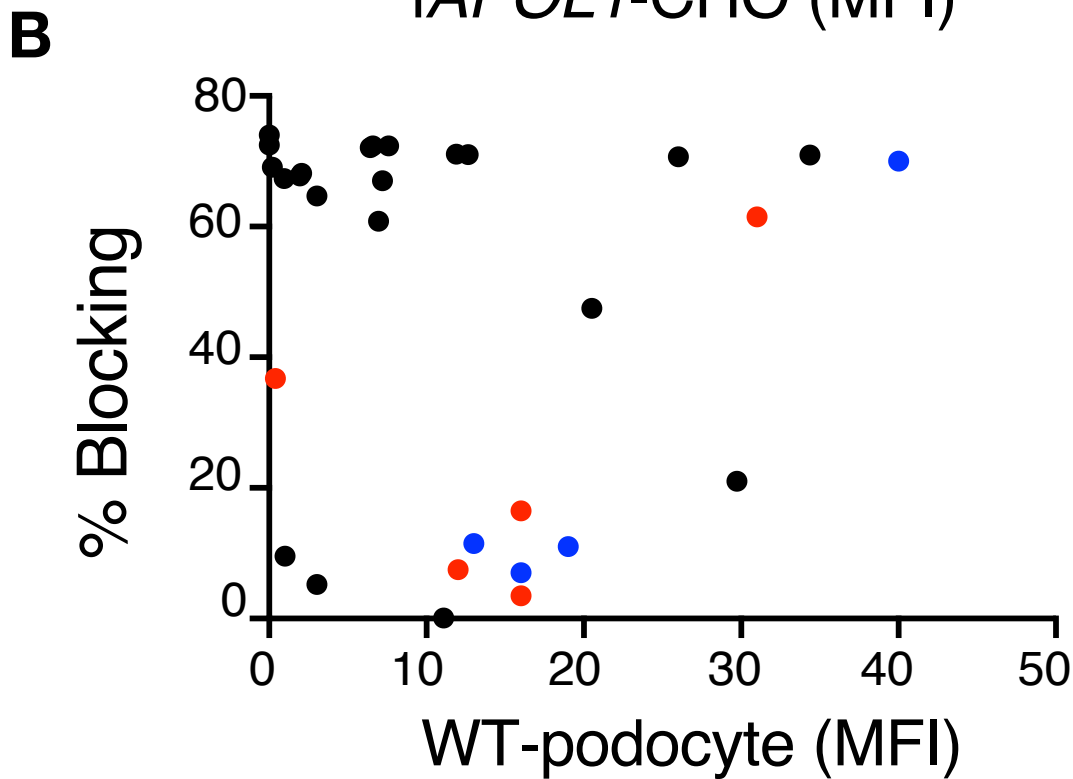
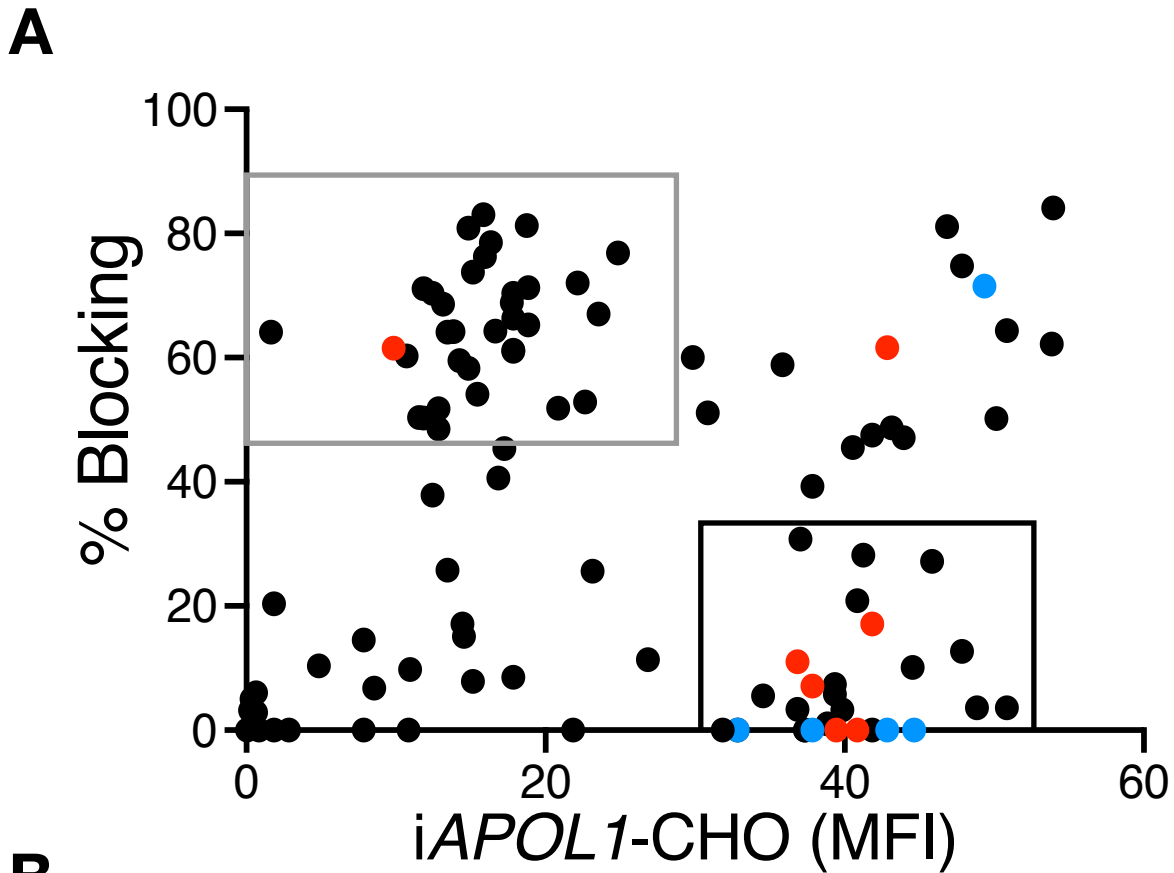
Supplemental Figure 8



Supplemental Figure 8. Immunoprecipitation of APOL1 from NHS with a different set of APOL1 antibodies confirms only blockers immunoprecipitate APOL1.

As in Figure 6D, all the blocking antibodies (A) could immunoprecipitate APOL1, except the conformational antibody 3.7F5, which is a poor blocker. By contrast (also as in Figure 6D) none of the non-blockers pulled down APOL1 (B); the blocking antibody 3.7D6 was included in the last lane as a positive control. (C) A subset of blocking and non-blocking antibodies was used to determine if HPR was co-immunoprecipitated with APOL1; HPR indeed showed the same pattern as APOA1 pull-down by the blocking antibodies.

Supplemental Figure 9

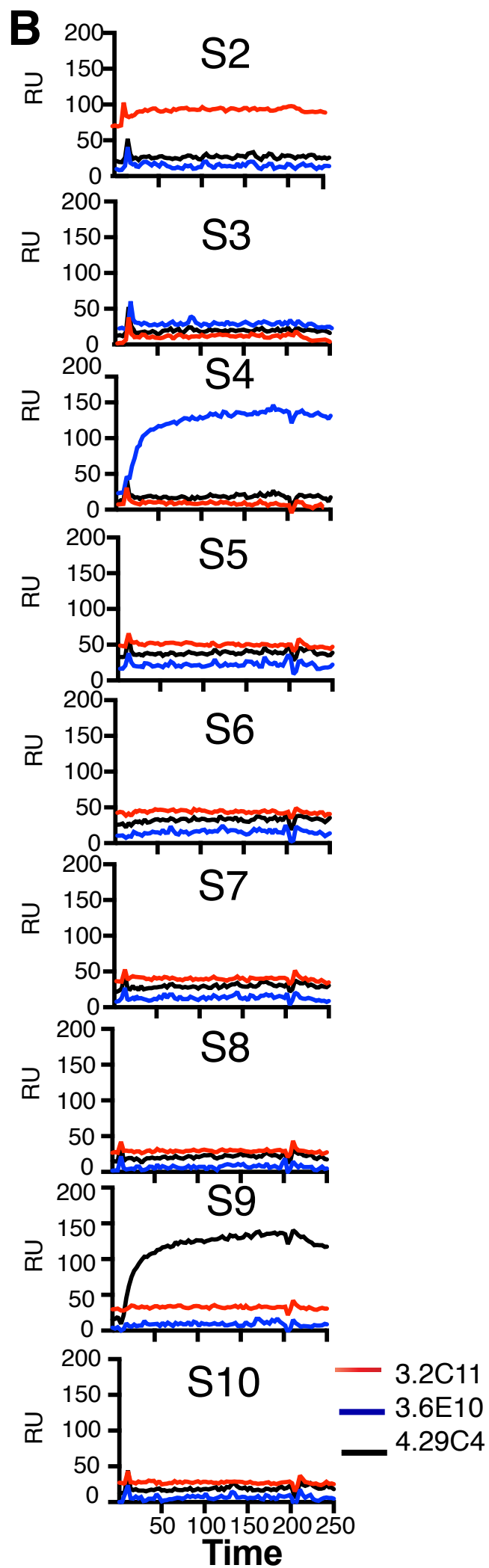
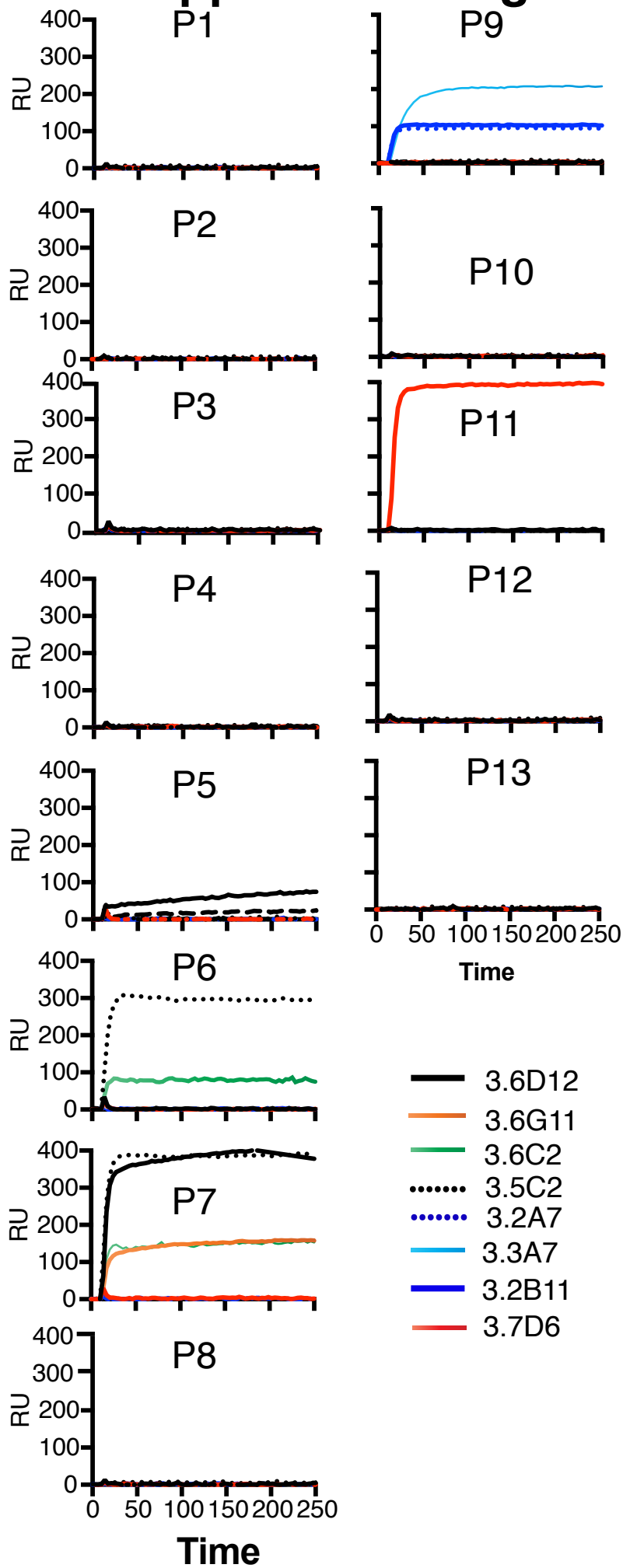


Supplemental Figure 9. Lack of correlation between surface APOL1 recognition and trypanolytic blockade by anti-APOL1 antibodies.

A) The percentage of trypanolysis blocking of each antibody (all 105 hybridomas from Method #3) at 1 $\mu\text{g/ml}$ is plotted versus its mean fluorescence intensity (MFI) on *iAPOL1*-CHO (construct a of Figure 1A) at the same concentration. Each dot represents an individual antibody. The correlation between surface binding and trypanolysis blockade is poor, since ~20 non-blocking antibodies were able to recognize APOL1 well by FACS (black box) and conversely ~20 strong blockers only weakly recognized APOL1 on CHO cells (MFI <20; grey box). The FACS data is representative of 2 individual experiments and the blocking data is the mean of 2 experiments. Blue dots represent antibodies mapped to region 131-150 and red dots indicate antibodies mapped to region 111-130 (see Figure 7 and Supplemental Figures 10 and 11).

B) As in (A) but with WT podocytes, replotting the data from Figure 5A and 5C (means of $n=3$). The trypanolytic blocking activity similarly does not correlate with binding to WT podocytes.

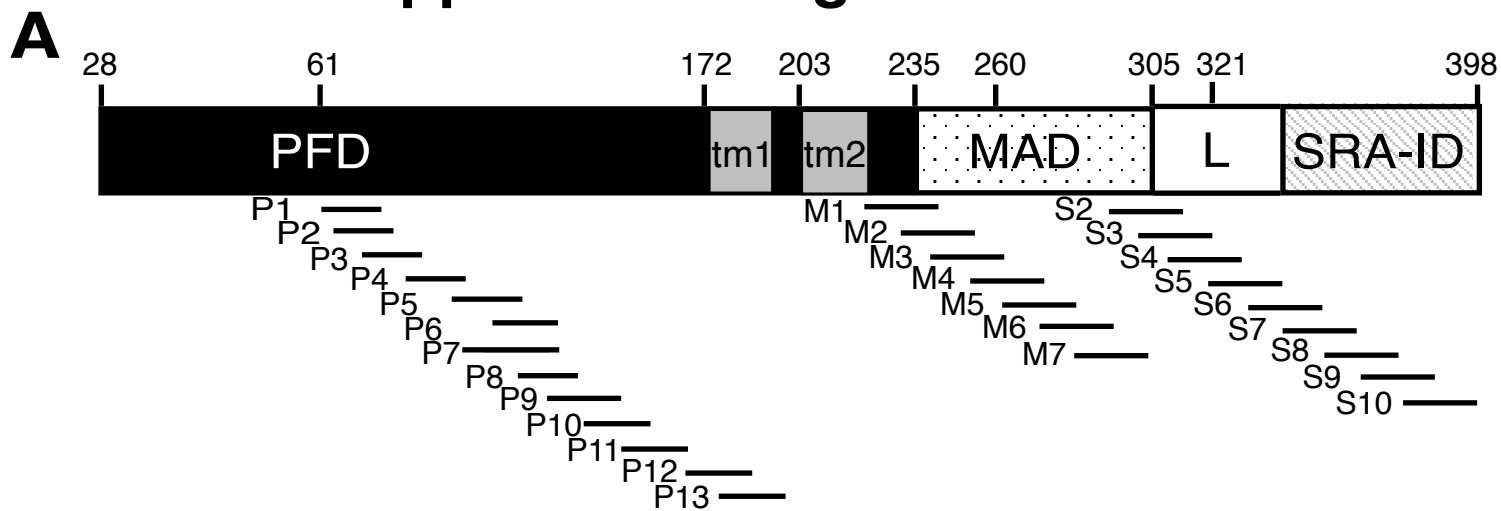
Supplemental Figure 10



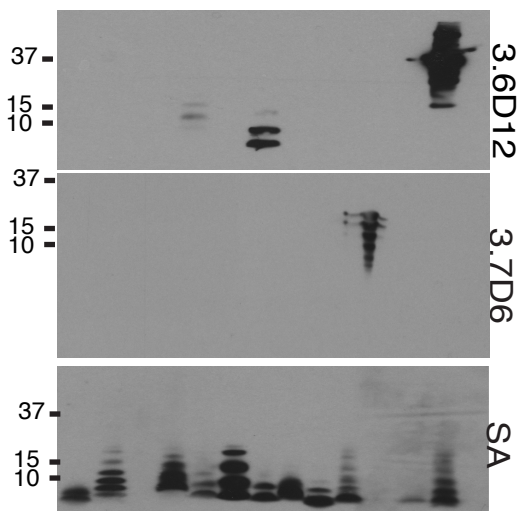
Supplemental Figure 10. Eleven anti-APOL1 antibodies were precisely mapped by surface plasmon resonance on overlapping peptides spanning the length of APOL1.

Examples of SPR measurements of fluid phase peptide (~20-mer peptides, listed in Supplemental Figure 11) binding to immobilized phase monoclonal anti-APOL1 antibodies using Catterra is shown for PFD and SRA-ID antibodies on PFD (A) or SRA-ID (B) peptides. The MAD antibodies were all negative by this method and are thus not shown.

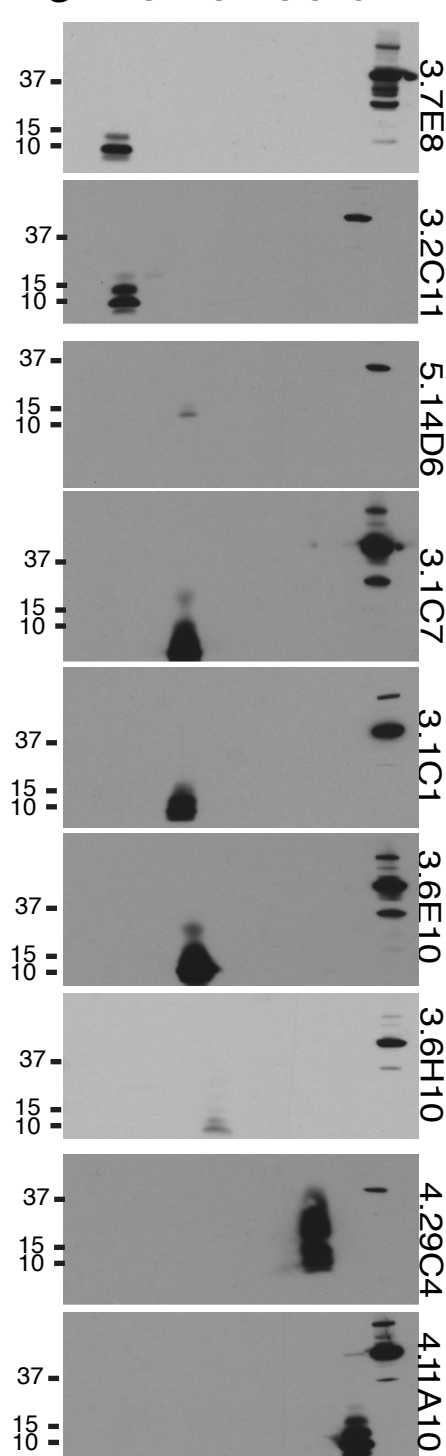
Supplemental Figure 11



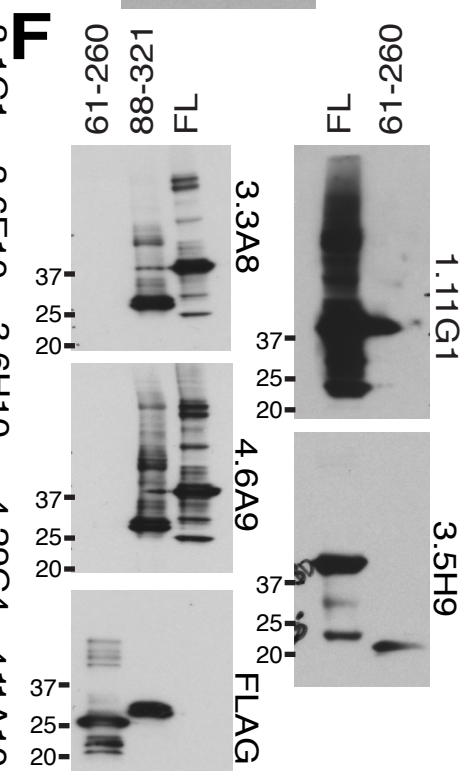
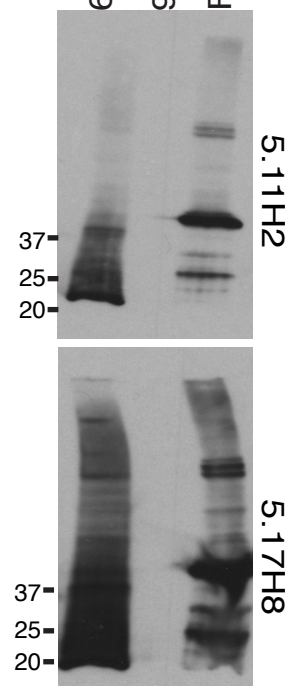
B P1 2 3 4 5 6 7 8 9 ¹⁰ ¹² 11 13 FL



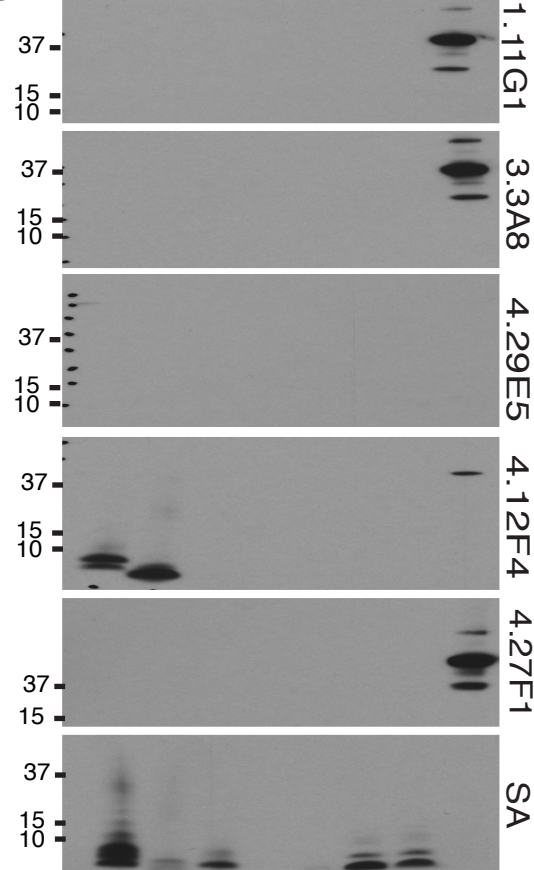
D S 2 3 4 5 7 8 9 10 FL



E 61-203 92-321 FL



C M 1 2 3 4 5 6 7 FL



Supplemental Figure 11. Successful epitope mapping of 18 anti-APOL1 antibodies by western blotting of short overlapping peptides covering the whole protein.

A) Schematic of APOL1 protein with the overlapping ~20-mer peptides along its length indicated below as black lines. P denotes PFD peptides, M the MAD and S the SRA-ID, and peptides were numbered sequentially for each domain.

B-D) Examples of domain mapping by Western blotting on the above peptides. Most PFD (B) and MAD (C) antibodies were negative on these peptides, which could be due to high oligomerization of these peptides or longer or non-linear epitopes for these antibodies. SRA-ID antibodies (D) bound well to their cognate peptides, indicating linear epitopes; note peptide S6 was not loaded due to insolubility. SA, streptavidin-HRP control to determine which peptides are detectable on the blots. FL, full length recombinant APOL1 control (aa 61-398).

E,F) Western blots with Sf9 lysates expressing FLAG-tagged truncated *APOL1* helped determine the broader domain for some of the PFD (E) and MAD (F) antibodies. FLAG, anti-FLAG antibody for FLAG-tagged truncated constructs.